

Novel methodology for the quantitative assay of fissile materials using temporal and spectral β -delayed γ -ray signatures

D.H. Chivers^a, K. Alfonso^a, B.L. Goldblum^{a,b,*}, B. Ludewigt^c

^a Department of Nuclear Engineering, University of California, Berkeley, CA 94720, USA

^b Department of Nuclear Engineering, University of Tennessee, Knoxville, TN 37996, USA

^c Lawrence Berkeley National Laboratory, Berkeley, CA 94720, USA

ARTICLE INFO

Article history:

Received 15 December 2010

Received in revised form 7 April 2011

Available online 18 May 2011

Keywords:

Delayed γ -rays

Active interrogation

Fission reactions

ABSTRACT

An analytical model for the generation of β -delayed γ -ray spectra following thermal-neutron-induced fission of mixed samples of ^{235}U and ^{239}Pu is presented. Using an energy-dependent figure-of-merit to designate the spectral regions employed in the assay, the unique temporal β -delayed γ -ray signatures are utilized to determine the fraction of ^{239}Pu in a mixed U–Pu sample. By evaluating the β -delayed γ -ray temporal signatures of both ^{235}U and ^{239}Pu within a 3 keV energy bin, traditional sources of systematic uncertainty in quantitative assay using β -delayed γ -ray signals, such as self-attenuation of the sample and energy-dependent γ -ray detection efficiency, are significantly reduced. The effects of the time-dependent Compton-continuum and growth of longer-lived nuclides on the quantitative assessment are explored. This methodology represents a promising extension of the conventional means of analysis for quantitative assay of fissile materials using β -delayed γ -ray signatures.

© 2011 Elsevier B.V. All rights reserved.

1. Introduction

There has been increased interest in recent years in the nondestructive assay of samples of fissile material for the purpose of quantifying ^{239}Pu material content [1–4]. The spectral dependence of β -delayed γ -rays emitted from decaying fission products of ^{235}U and ^{239}Pu has been established experimentally for time scales on the order of seconds to minutes [5]. Traditionally, a sample of fissile material is interrogated with neutrons or photons and the relative intensities of the β -delayed γ -rays emitted from fission fragments and their decay daughters are used to quantify the fissile material constituents in the sample [6–8]. Attenuation of the emitted γ -rays within the sample and γ -ray detection efficiency will bias the determination of the relative intensities of the β -delayed γ -ray lines unless these effects are known a priori and can be accounted for [9]. The minimization of the range between the energy regions used in forming intensity ratios can reduce, but never fully eliminate, this systematic bias. The method presented here provides an approach independent of intensity ratios via analysis of the temporal response of emitted β -delayed γ radiation from fissile materials. This is accomplished by normalizing the information contained in spectral intensity differences

such that only temporal differences remain. The temporal response differences are only affected by the initial population of fission products and associated lifetimes and not by self-attenuation of the sample.

An analytical modeling effort was employed to generate β -delayed γ -ray spectra as a function of time following pulsed thermal neutron interrogation of both pure and mixed samples of ^{239}Pu and ^{235}U . Regions of interest in the energy-time domain were established for identification of the relative ^{239}Pu and ^{235}U content in a mixed sample. The fraction of the intensity-normalized β -delayed γ -ray signal over an optimized time interval was sampled using Gaussian statistics to determine the proportion of ^{239}Pu in a mixed U–Pu sample and associated measurement variance. The basic principles of the temporal β -delayed γ -ray approach are outlined in Section 2, while Section 3 provides a description of the model development and utilization. Within a practical implementation, long-lived nuclide build-up and Compton scatter reduces the sensitivity of the technique. The results for inversion computation with stochastic effects for the ideal, long-lived nuclide build-up, and Compton scatter cases are provided in Section 4. Concluding remarks are given in Section 5.

2. Theory

Thermal neutron-induced fission of ^{235}U and ^{239}Pu produces a well-characterized direct fission product yield [10]. The chain yield

* Corresponding author at: Department of Nuclear Engineering, University of Tennessee, Knoxville, TN 37996, USA. Tel.: +1 510 642 5760; fax: +1 510 643 9685.
E-mail address: goldblum@utk.edu (B.L. Goldblum).

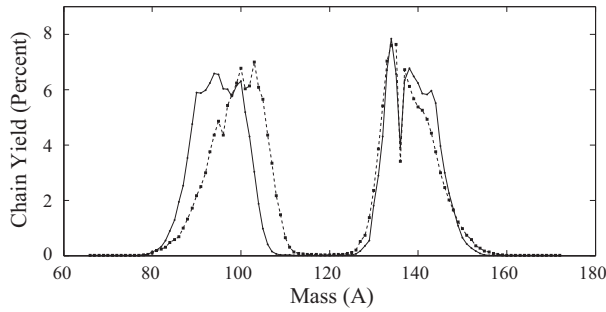


Fig. 1. Thermal fission fragment chain yield mass distribution for ^{235}U (solid line) and ^{239}Pu (dashed line) [10].

of secondary¹ fission fragments (i.e., the percent of fissions which, after prompt neutron emission, result directly in production of an isotope of mass A) resulting from the thermal fission of ^{235}U and ^{239}Pu is illustrated in Fig. 1. Radioactive decay of the fission fragments produces a decay chain, where the progeny, if radioactive, build up and/or die away as time progresses. The difference in the β -delayed γ -ray intensities arises from the difference in the independent yields of the fission fragments (i.e., the fraction of fissions which, after prompt neutron emission, results directly in that isotope). Fission fragments comprising the light-mass peak ($A \approx 80 - 110$) and regions of the heavy-mass peak ($A \approx 137 - 144$), as shown in Fig. 1, are likely to have sufficiently disparate independent yields in the thermal fission of ^{235}U and ^{239}Pu such that the spectral dependence of the β -delayed γ -ray signatures from the decay daughters is clearly distinguishable for the two fissile isotopes.

The differences in the independent yields can be observed in both the differences in the intensity and temporal distributions of the γ -ray emission. For a given γ -deexcitation of energy E_γ , the peak region count-rate, R , may be expressed as the product of the γ -ray emission rate, the detector peak efficiency, and the self-attenuation factor:

$$R(E_\gamma, t) = N(t) * \lambda * I_\gamma * \varepsilon_V(0, E_\gamma) * F_V(\mu, E_\gamma), \quad (1)$$

where $N(t)$ is the amount of the nuclide at time t , λ is the decay constant of the nuclide, I_γ is the γ -ray yield and $\varepsilon_V(0, E_\gamma)$ is the detector peak efficiency with no self-attenuation of the sample. The self-attenuation factor, $F_V(\mu, E_\gamma)$ is defined as

$$F_V(\mu, E_\gamma) = \frac{\varepsilon_V(\mu, E_\gamma)}{\varepsilon_V(0, E_\gamma)}, \quad (2)$$

where $\varepsilon_V(\mu, E_\gamma)$ is the detector peak efficiency given self-attenuation with an average attenuation coefficient, μ [11]. In the limit of small sample size, $F_V(\mu, E)$ will approach unity and differences in the total intensity of peak energy regions can be mapped directly to differences in fission product yields, and thus, to fissile nuclide content. However, if the sample provides appreciable attenuation differences for the γ -rays of interest and this effect is unknown a priori, then a systematic bias is introduced. The magnitude of this systematic error is dependent upon sample composition, geometry and homogeneity, and may be reduced by the analysis of γ -rays close in energy as to reduce the difference in the self-attenuation factors. Peak ratio methods suffer the practical limitation of the energy resolution of the detector, however, one can utilize temporal differences within a single energy region (whose width may be defined to be on the order of the energy resolution of the detector) to quantify differences in the fissile material content.

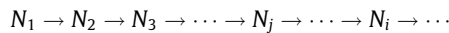
¹ For simplicity, fission fragments are considered after prompt neutron emission throughout the remainder of the text unless otherwise noted.

Differences in the temporal distribution of γ -ray emission arise from differences in the independent yields of the nuclides in the decay chain(s) that give rise to the nuclide or nuclides that produce the dominant γ -ray(s) in the energy bin of interest. An example of this phenomenon is given at the end of Section 3. For the cases in which there is only one dominant γ -deexcitation in a given energy bin that gives rise to a disparate temporal response for ^{235}U and ^{239}Pu , the dominant nuclide is either produced from different fission fragments and/or stems after branching from multiple decay chains. In this case, a variation in temporal evolution may occur and the observation is independent of sample attenuation. When the energy range of interest contains dominant γ -ray emissions from two or more nuclides, the attenuation bias is minimized by utilizing γ -ray emissions that are closer in energy than the energy resolution of the detector. It should be noted that this does not reduce attenuation bias to zero, but only minimizes it via analysis of γ -ray emissions that are close in energy.

3. Methodology

In order to estimate the temporal response, a model was developed to predict the probability distribution of β -delayed emission of γ -rays in the energy-time domain using a fine binning of 3 keV and 50 ms. Each of the energy bins were intensity-normalized in order to produce probability distributions in time. Although higher-order shape components of the response distributions contain information, any practical implementation will be dominated by the first-order component due to statistical effects.

Consider the following general case of a linear radioactive decay chain:



Initially, an algorithm was employed to determine the isotopes included in a given decay chain. The half-life, decay mode(s), and corresponding branching ratio(s) for the first isotope in the decay chain, N_1 , were compiled. A branching ratio threshold of 0.01% was applied such that daughter nuclides with branching ratios of less than 0.01% were omitted from the decay chain, along with their associated γ -rays and decay daughters. It is assumed that these nuclides do not significantly contribute to the time-dependent β -delayed γ -ray signal. The daughter isotope, N_2 , was determined by the decay mode(s) of the first isotope in the decay chain, N_1 , and again the associated decay data were compiled. This compilation of decay daughters and associated decay data proceeded iteratively until the nuclide(s) at the end of the chain(s) were stable with respect to radioactive decay. Due to limited decay data, the long-lived isotopes listed in Table 1 were designated as stable. This is reasonable given that the time-scale considered for this analysis is on the order of seconds. The decay data, which includes the half-life,

Table 1

Long-lived isotopes designated as stable. The uncertainty given is in the least significant digit(s).

Isotope	Half-life (years)	Uncertainty
^{70}Zn	$> 5 \times 10^{14}$	
^{82}Se	1.08×10^{20}	$+26$ -6
^{96}Zr	$> 3.8 \times 10^{19}$	
^{100}Mo	1×10^{19}	± 10
^{128}Te	2.2×10^{24}	± 3
^{130}Te	7.9×10^{20}	± 10
^{136}Xe	$> 2.36 \times 10^{21}$	
^{142}Ce	$> 5 \times 10^{16}$	
^{150}Nd	1.1×10^{19}	
^{149}Sm	$> 2 \times 10^{15}$	

decay mode(s), and corresponding branching ratio(s), are obtained from the updated nuclear decay libraries of the CINDER 2008 actinide transmutation code package [12], the Table of Radioactive Isotopes (TORI) [13], the Sigma nuclear reaction database [14] and the Evaluated Nuclear Structure Data File (ENSDF-2) [15].

Assuming fission occurs at $t = 0$, the amount of any nuclide, i , in the decay chain, N_i , present at time t , was determined by the generalized batch-decay Bateman equation [16]:

$$N_i = \sum_{\ell=1}^{i-1} \left[N_{\ell}^0 \xi_{\ell} \xi_{\ell+1} \cdots \xi_{i-1} \sum_{j=\ell}^i \frac{e^{-\mu_j t}}{\prod_{k=\ell, k \neq j} (\mu_k - \mu_j)} \right] + N_i^0 e^{-\mu_i t}, \quad (3)$$

where the ξ terms are the partial radioactive decay constants, the μ terms are the full radioactive decay constants, and N_{ℓ}^0 and N_i^0 are the initial amount of the ℓ th and i th nuclides in the chain, respectively. The partial radioactive decay constant, ξ_i , for the i th isotope was calculated by multiplying the full decay constant for the i th isotope, μ_i , by the corresponding normalized branching ratio for decay into the $(i + 1)$ th isotope, as shown below:

$$\xi_i = \mu_i \frac{\Gamma_{i+1}}{\Gamma_{tot}}, \quad (4)$$

where Γ_{i+1} is the partial width for decay into the $(i + 1)$ th isotope and Γ_{tot} is the sum of the decay probabilities for all allowed decay modes.

The irradiation period was simulated using a δ -pulse of neutrons at $t = 0$. For the initial irradiation, fission product independent yields from England and Rider [10] were taken as initial conditions. In the event of a branched radioactive decay chain, the amount of the i th nuclide in the decay chain at time t , $N_i(t)$, was obtained by summing the amounts generated from the individual linear chains. If a nuclide was present in the decay chain of multiple fission fragments, the amount of that nuclide was obtained from the sum of the various $N_i(t)$ values from different decay chains. The counting interval spanned 10 s. The total amount of a given nuclide (in units of atoms per 10^3 fissions) at the end of the counting interval was then added to the fission product yields from England and Rider. This sum was utilized as initial conditions in Eq. (3) and thus began the next irradiation and counting cycle.

To generate the time-dependent γ -ray spectra, it was assumed that the amount of any given nuclide at some time t^* after fission, $N_i(t^*)$, is constant over a time bin, $\Delta t = 50$ ms, and the k th γ -decay line, $\Psi_{i,k}(E_{\gamma}^k, t^*)$, was then generated for each γ -ray from the decay of N_i using the following equation:

$$\Psi_{i,k}(E_{\gamma}^k, t^*) = N_i(t^*) * \lambda_i * I_{\gamma}^k * \Delta t. \quad (5)$$

Here, the k index designates each individual γ -deexcitation of N_i , λ_i is the decay constant of N_i and I_{γ}^k is the intensity of the k th γ -ray with energy E_{γ}^k . A single fission fragment or decay daughter with index i has k_{max} $\Psi_{i,k}$ values associated with it (i.e., k_{max} is the maximum number of γ -rays emitted in the deexcitation of N_i). Here, the steady-state approximation is employed (i.e., the amount of the i th nuclide, N_i , is assumed to not change significantly over the time bin, Δt). This is reasonable if the half-lives for the decay processes governing the production and removal of the i th nuclide are long when compared with the time bin, Δt . The $\Psi_{i,k}(E_{\gamma}^k, t^*)$ values were subsequently convolved with a Gaussian function of the form

$$G(E) = \frac{1}{\sigma\sqrt{2\pi}} e^{-\frac{(E-E_{\gamma})^2}{2\sigma^2}}, \quad (6)$$

where E_{γ} represents the centroid of the peak, and

$$\sigma(E_{\gamma}) = \frac{\sqrt{F\epsilon E_{\gamma} + W_E^2}}{2.35}. \quad (7)$$

Here, F is the Fano factor of the detector, assumed to be 0.129 in this case, ϵ is 2.96 eV, the average energy required to create an electron-hole pair in germanium, and W_E^2 represents the broadening effects due to electronic noise, approximated as $(2.07 \text{ keV})^2$ [17].

The effect of the time-dependent Compton continuum was also explored. Two scenarios for γ -ray detection were considered: an idealized case, in which effects of the Compton continuum were neglected, and detection via an ORTEC GEM-10175 coaxial high-purity Germanium (HPGe) detector (dia. = 46.3 mm, $l = 44.2$ mm) with a relative efficiency of 10% at 1.33 MeV. The low efficiency detector was chosen for modeling a planned experiment; though not required, high efficiency HPGe detectors are greatly preferred for the measurements discussed here. For the latter scenario, Monte Carlo simulations [18] were employed to determine the area of the Compton continuum, as well as photopeak, single- and double-escape peak efficiencies, in intervals of 100 keV. The area of the Compton-continuum and peak detection efficiencies were fit with six-order polynomials over an energy range of 1–7 MeV and interpolation was accomplished for each $\Psi_{i,k}$ γ -deexcitation of N_i . The Compton-continuum was incorporated into the spectra using a constant-intensity shelf-model terminating at the Compton edge.

Possible sources of error in the time-dependent β -delayed γ -ray spectra generated with this model include:

- (i) treatment of the neutron irradiation period as a δ -pulse in time. In a practical experimental scenario, neutron irradiation will continue for a fixed time period and fission fragments will be generated over the entire irradiation period. However, if the irradiation period is short with respect to the time constants for decay and growth of the isotopes of interest, it is reasonable to neglect continuous production of fission fragments over the irradiation period.
- (ii) modeling of the Compton-continuum shape as a shelf that terminates at the Compton edge. Although single- and double-escape peaks were included in the model, structure may be present in the Compton-continuum, particularly in the energy range near these escape peaks. Omission of the detailed structure of the Compton-continuum is not expected to affect the overall conclusions presented here.
- (iii) incomplete or inaccurate fission product independent yields and/or decay libraries. The results of this study are limited by the accuracy of the available nuclear data.

Further, it is important to note that as the number of irradiation and counting cycles increases, the growth of long-lived nuclides will affect the quantitative sample assessment based on the temporal dependence of the β -delayed γ -ray signal. To investigate this, we consider the time-dependent β -delayed γ -ray spectrum generated after a single thermal neutron irradiation and compare this to the spectrum generated after 1001 irradiation and counting cycles, as described in detail in Section 4.

For pure samples of both ^{235}U and ^{239}Pu , β -delayed γ -ray spectra were generated after a single irradiation and counting cycle, denoted $N^{25}(t)$ and $N^{49}(t)$, respectively. For each 3 keV γ -ray energy bin, the pure ^{235}U and ^{239}Pu β -delayed γ -ray signals were normalized as a function of time over the entire counting interval, denoted $N_{norm}^{25}(t)$ and $N_{norm}^{49}(t)$, respectively. The fraction of the normalized response over a time interval from 0 to t_x s, where $t_x \leq 10$ s, was obtained for both pure ^{235}U and ^{239}Pu signals, defined as

$$F^{25} = \int_0^{t_x} N_{norm}^{25}(t) dt \quad (8)$$

and

Table 2

The top-ten energy bins, listed by bin centroid, with the highest FOM. The energy bin width is 3 keV.

Energy bin centroid (keV)			
Single neutron pulse		1001 neutron pulses	
Idealized	Compton	Idealized	Compton
1217.5	1217.5	1217.5	1217.5
2240.5	1256.5	1259.5	1904.5
1256.5	1259.5	1265.5	1259.5
2435.5	2441.5	1907.5	1220.5
2942.5	1589.5	1220.5	1256.5
2438.5	2240.5	1592.5	1907.5
2441.5	2942.5	1514.5	1091.5
1142.5	1043.5	2435.5	1103.5
2939.5	1169.5	2438.5	1043.5
1760.5	1583.5	1904.5	1088.5

$$F^{49} = \int_0^{t_x} N_{norm}^{49}(t) dt, \quad (9)$$

respectively. The t_x parameter was determined dynamically for each 3 keV energy bin by optimizing the figure-of-merit (FOM) associated with the signal, defined as

$$FOM(E_\gamma) = \frac{|F^{25} - F^{49}|}{\sqrt{F^{25} + F^{49}}} \sqrt{T^{25} + T^{49}}. \quad (10)$$

The first factor in the product on the right-hand-side of the equation represents the signal-to-noise in the assessment, where the numerator (signal) is the difference in the fraction of counts for pure ^{235}U and ^{239}Pu obtained in the time interval from 0 up to t_x s and the denominator (noise) is obtained using traditional counting statistics. The second multiplicand in the product is a statistical factor used to scale the signal-to-noise based upon the intensity of the non-normalized responses, where

$$T^{25} = \int_0^{t_x} N^{25}(t) dt \quad (11)$$

and

$$T^{49} = \int_0^{t_x} N^{49}(t) dt. \quad (12)$$

It is important to note that the t_x determination and FOM ranking is based upon assessment of a sample with no a priori knowledge of the fractional ^{239}Pu content. That is, the FOM assumes a linear scaling of the normalized fraction of the β -delayed γ -ray response as a function of ^{239}Pu content in the sample. This is further discussed in Section 4.1.

For both a single neutron irradiation and after 1001 neutron pulses, the energy of the top-ten-ranked energy bins for the idealized and Compton-included scenarios are given in Table 2. The β -delayed γ -ray signals in the top-ranked energy bin of 1217.5 ± 1.5 keV, following a single neutron irradiation for pure samples of ^{235}U and ^{239}Pu , are illustrated by the bold solid lines in Fig. 2(a) and (b), respectively. The strongest contributing fission products to the total spectral intensity are ^{92}Kr (thin solid line, $t_{1/2} = 1.85$ s) and ^{137}I (dotted line, $t_{1/2} = 24.5$ s). The latter comprises more than 10% of the total signal in the temporal region extending from 0 to t_x s for the ^{239}Pu response only, but is present in the ^{235}U response as a non-dominant contributor (dashed line). The contribution from non-dominant nuclides in both Fig. 2(a) and (b) is roughly linear over the entire temporal region probed.

The fission fragments responsible for the ^{92}Kr and ^{137}I fission products are ^{92}Se , ^{94}Se , ^{92}Br , ^{93}Br , and ^{92}Kr , for the ^{92}Kr isotope, and ^{137}Sn , ^{137}Sb , ^{138}Sb , ^{139}Sb , ^{137}Te , ^{138}Te and ^{137}I , for the ^{137}I isotope, where ^{92}Kr and ^{137}I could be formed both directly after fission

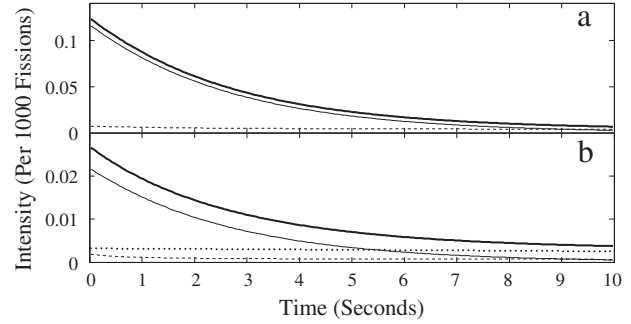


Fig. 2. The idealized β -delayed γ -ray response in intensity per 10^3 fission events as a function of time, obtained for a pure sample of (a) ^{235}U and (b) ^{239}Pu , are represented by the bold solid lines for the top-ranked energy bin of 1217.5 ± 1.5 keV. The solid and dotted lines correspond to the contributions from ^{92}Kr and ^{137}I , respectively. The dashed line represents the cumulative contribution of all other nuclides that contribute to the total signal, but comprise less than 10% of the total signal in the temporal region extending from 0 to t_x s, where t_x is equal to 2.525 s.

(after prompt neutron emission) or through the decay of other nuclides. As expected from the thermal fission fragment chain yield mass distribution for ^{235}U and ^{239}Pu (see Fig. 1), the corresponding fission fragments have a mass number A in the range from 92–94 and 137–139. The difference in β -delayed γ -ray time signatures arises from the disparate fission fragment independent yields of the nuclides in the decay chains (listed above) that give rise to ^{92}Kr and ^{137}I (i.e., those isotopes that provide a dominant contribution to the γ -ray spectrum in this energy bin).

4. Results

To generate the β -delayed γ -ray spectrum for a mixed sample of ^{235}U and ^{239}Pu , the raw, non-normalized ^{235}U and ^{239}Pu β -delayed γ -ray signals are combined fractionally, as follows:

$$N^{\text{mix}}(t) = \xi[(1-f)N^{25}(t) + fN^{49}(t)], \quad (13)$$

where ξ is a factor representing the total number of fission events and f is the fraction of ^{239}Pu in the sample. Because a specific neutron energy spectrum was not assumed, the above treatment neglects the fission cross sections for ^{235}U and ^{239}Pu . In practice, the β -delayed γ -ray spectra obtained from the analytical model in units of intensity per 10^3 fissions must be scaled by the energy-dependent fission cross section integrated over the relevant neutron energy spectrum. For the top-fifty 3 keV energy bins, as determined by the FOM ranking, the mixed signal, $N^{\text{mix}}(t)$ is normalized over the 10 s interval and integrated over the temporal region up to the t_x value associated with that energy bin. The signal is defined as a Gaussian sampling of the fraction of the normalized response over a time interval from 0 up to t_x s. That is,

$$F^{\text{mix}} = \frac{\int_0^{t_x} N^{\text{mix}}(t) dt}{\int_0^{10\text{s}} N^{\text{mix}}(t) dt}. \quad (14)$$

For the top-fifty energy bins, as determined by the FOM ranking, with $\xi = 10^6$, the normalized fraction of the β -delayed γ -ray spectrum for a mixture of ^{235}U and ^{239}Pu , determined over a time interval from 0 up to the associated t_x value, was sampled with Gaussian statistics for 10,000 trials. That is, a single trial consists of sampling all of the top-fifty energy bins once and solving for the normalized fraction. A number of identical trials were obtained to provide the expected variance in the measurement. Based upon the normalized fraction of the β -delayed γ -ray spectrum, an assessment of the ^{239}Pu fraction in the mixed sample, as well as the associated uncertainty, is obtained.

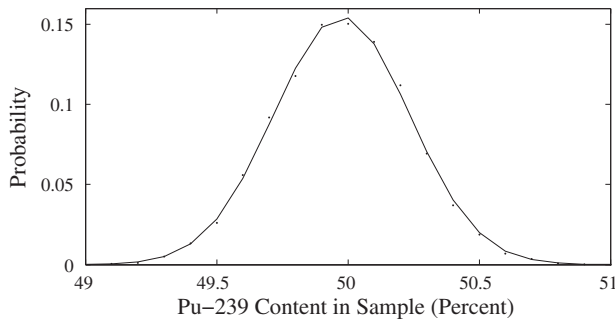


Fig. 3. The probability of determining a given ^{239}Pu sample content, in percent, from spectral data in the top-fifty-ranked energy bins obtained via a single neutron irradiation, neglecting the effects of Compton scattering. The solid line is a Gaussian fit of the data with a mean of 49.98% and a FWHM of 0.61%.

4.1. Idealized case for a single δ -pulse of neutrons

The probability for obtaining a given normalized fraction of the β -delayed γ -ray spectrum in the top-ranked 1217.5 ± 1.5 keV energy bin via a single neutron irradiation, neglecting Compton scattering, was sampled with Gaussian statistics for 10,000 trials. The normalized fraction of the β -delayed γ -ray signal was determined for a 50% mixture of ^{235}U and ^{239}Pu , integrated over a time interval from 0 up to the t_x value of 2.525 s. A Gaussian fit of the sampled data with a mean, \bar{x} , of 0.568 and a full width at half maximum (FWHM) of 0.001 was obtained. The normalized fraction of the mixed β -delayed γ -ray signal was utilized to determine the percentage of ^{239}Pu in a mixed sample. This process was repeated for the top-fifty-ranked energy bins and the probability for determining a given ^{239}Pu fractional sample content, as obtained from the β -delayed γ -ray spectral data via a single neutron irradiation, neglecting the effects of Compton scattering, is illustrated in Fig. 3. The data points represent a sampling with 10,000 trials for a 50% mixture of ^{235}U and ^{239}Pu . The solid line is a Gaussian fit of the sampled data with $\bar{x} = 49.98\%$ and $\text{FWHM} = 0.61\%$. This corresponds to a ^{239}Pu content in the sample of $49.98 \pm 0.26\%$, representing excellent agreement with the 50% ^{239}Pu sample content in the simulated β -delayed γ -ray spectral response for an idealized, single irradiation scenario. The analysis was repeated for a mixed U–Pu sample of 10% ^{239}Pu and 90% ^{239}Pu with assessed ^{239}Pu sample contents of $9.97 \pm 0.36\%$ and $89.99 \pm 0.17\%$, respectively.

Fig. 4(a) showcases the variation in the normalized fraction of the mixed β -delayed γ -ray signal as obtained from the temporal signal in the 1217.5 ± 1.5 keV energy bin as a function of the percentage of ^{239}Pu in a mixed sample. As mentioned above, ranking of the top energy bins for assessment of the temporal and spectral dependence of the β -delayed γ -ray signal via the FOM is based upon the assumption of linear scaling of F^{mix} with the fractional ^{239}Pu sample content. However, as indicated in Fig. 4(a), non-linearities exist in the normalized fraction of the mixed β -delayed γ -ray spectrum as a function of the percentage of ^{239}Pu in a mixed sample. Here, the curvature of the normalized fraction of the mixed β -delayed γ -ray spectrum as a function of the percentage of ^{239}Pu is greater for high ^{239}Pu content. That is, for this energy bin and simulated data, the non-linearities result in a more accurate assessment for high ^{239}Pu content samples.

Now consider, in contrast, the normalized fraction of the β -delayed γ -ray response obtained from an idealized, single irradiation for the 2240.5 ± 1.5 keV and 2699.5 ± 1.5 keV energy bins as a function of ^{239}Pu sample content, graphically illustrated in Fig. 4(b) and (c), respectively. Fig. 4(b) shows a roughly linear relationship between the normalized fraction of the mixed β -delayed γ -ray signal as a function of the percentage of ^{239}Pu in a mixed

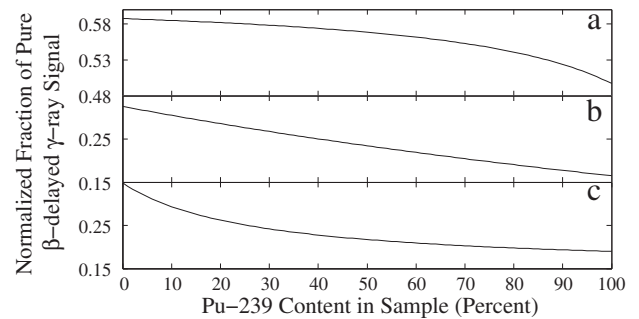


Fig. 4. The normalized fraction of the β -delayed γ -ray response obtained from a single pulse, idealized scenario for the (a) 1217.5 ± 1.5 keV, (b) 2240.5 ± 1.5 keV, and (c) 2699.5 ± 1.5 keV energy bins as a function of the percent of ^{239}Pu in a mixed sample. Note the zero-suppressed ordinate axes.

sample and thus, should provide reasonable assessment of the fractional ^{239}Pu content regardless of the sample composition. In contrast, Fig. 4(c) showcases a highly non-linear relationship between the normalized fraction of the mixed β -delayed γ -ray signal and the percentage of ^{239}Pu in a mixed sample, which would be more appropriate for assessment of low ^{239}Pu content samples. Given the possible non-linearities in the normalized fraction of the mixed β -delayed γ -ray signal as a function of the percentage of ^{239}Pu in a mixed sample, an iterative approach is suggested in which the value of the ^{239}Pu fraction in the mixed sample obtained from the first iteration is used to determine newly optimized values of t_x values and ranking of energy bins. The assessment is repeated until the derived percentage of ^{239}Pu in the mixed sample converges.

4.2. Effects of the Compton-continuum

The probability for determining a given ^{239}Pu fractional sample content, as obtained from the β -delayed γ -ray spectral data in the top-fifty-ranked energy bins via a single neutron irradiation, and including the effects Compton scattering, is illustrated in Fig. 5. The data points represent a sampling with 10,000 trials for a 50% mixture of ^{235}U and ^{239}Pu . The solid line is a Gaussian fit of the data with $\bar{x} = 47.38\%$ and $\text{FWHM} = 9.02\%$ and thus, we derive a fractional ^{239}Pu content in the sample of $47.38 \pm 3.84\%$.

The increased uncertainty in this assessment relative to the ideal scenario is due, in part, to the decreased intensity of the non-normalized, time-dependent, β -delayed γ -ray responses. For the top ranked energy bin of 1216–1219 keV and pure samples of both ^{235}U and ^{239}Pu after a single neutron irradiation, shown in Fig. 6(a) and (b), respectively, a decreased total β -delayed γ -

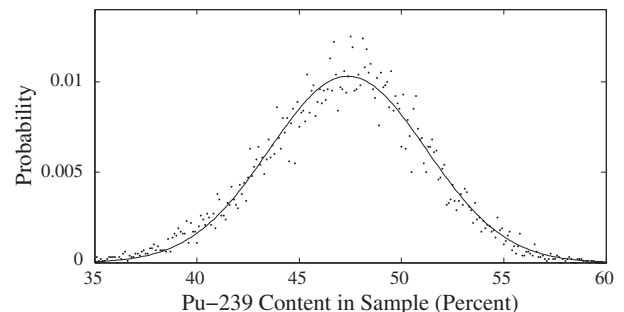


Fig. 5. The probability of determining a given ^{239}Pu sample content, in percent, obtained from a single neutron irradiation, with Compton effects included, obtained from the FOM-derived top-fifty-ranked energy bins. The solid line is a Gaussian fit of the data with a mean of 47.38% and FWHM of 9.02%.

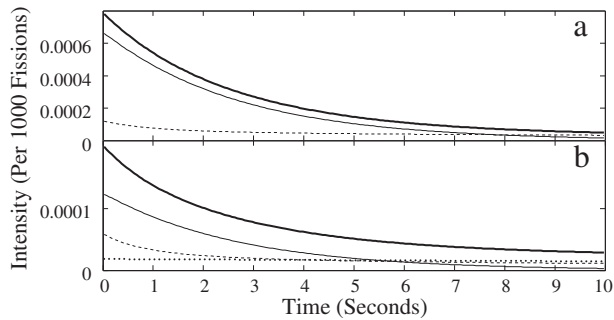


Fig. 6. The β -delayed γ -ray responses, including the effects of Compton scattering, in intensity per 10^3 fission events as a function of time, obtained for a pure samples of (a) ^{235}U and (b) ^{239}Pu after a single neutron irradiation, are represented by the bold solid lines. The solid and dotted lines correspond to the contributions from ^{92}Kr and ^{137}I , respectively. The dashed line represents the cumulative contribution of all other nuclides that contribute to the total signal, but comprise less than 10% of the total signal in the temporal region extending from 0 to t_x s.

ray intensity (solid bold line) is observed. Here, the strongest contributing fission products to the total spectral intensity are again ^{92}Kr (thin solid line) and ^{137}I (dotted line). However, the relative contribution of non-dominant nuclides (i.e., those nuclides that contribute to the signal, but comprise less than 10% of the total signal in the temporal region extending from 0 to t_x s, where t_x is equal to 2.675 s) is increased compared to the idealized, single neutron irradiation scenario illustrated in Fig. 2. For a single neutron irradiation, the number of nuclides present as non-dominant contributors in the idealized scenario is 187, compared to 216 non-dominant nuclides for the Compton-included scenario. Although the uncertainty in the assessment is larger due to the time-dependence of the Compton continuum, we still obtain agreement within one standard deviation with the simulated ^{239}Pu sample content of 50%. Nonetheless, the data suggest that Compton-suppression of the β -delayed γ -ray signals will result in a quantitative assessment of the ^{239}Pu sample content with decreased uncertainty. This could be accomplished, for example, by utilizing an annular bismuth germanate shield mounted at the rear face of the germanium crystal.

4.3. Effects of longer-lived nuclides

An assessment of the ^{239}Pu fractional sample content was repeated for both the idealized and Compton-included scenarios after 1001 neutron pulses (corresponding to approximately 2.8 h). Using the top-fifty-ranked energy bins, the normalized fraction of the mixed β -delayed γ -ray signal, obtained after 1001 irradiation and counting cycles, was utilized to determine the percentage of ^{239}Pu in a mixed sample. The probability distribution for assessing a given ^{239}Pu fractional sample content, neglecting the effects of Compton scattering, was obtained using a sampling of 10,000 trials for a 50% mixture of ^{235}U and ^{239}Pu . A Gaussian fit of the sampled data was obtained with $\bar{x} = 50.00\%$ and $\text{FWHM} = 0.38\%$. The assessed ^{239}Pu content in the sample of $50.00 \pm 0.16\%$ again represents excellent agreement with the simulated 50% ^{239}Pu sample content.

The effects of Compton scattering on the assessment of the ^{239}Pu fractional sample content was investigated following 1001 neutron irradiation and counting cycles. Using a sampling of 10,000 trials for a 50% mixture of ^{235}U and ^{239}Pu , a Gaussian fit of the data was obtained with $\bar{x} = 48.98\%$ and $\text{FWHM} = 5.99\%$. The derived fractional ^{239}Pu sample content of $48.98 \pm 2.54\%$ provides an accurate assessment of the simulated ^{239}Pu sample content of 50%. The decreased uncertainty in the assessment, relative to the Compton-included, single neutron irradiation scenario, is primarily

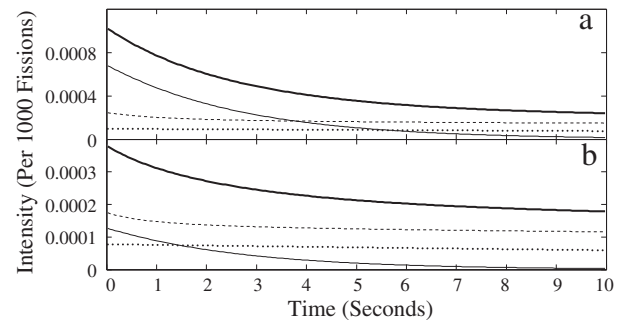


Fig. 7. The β -delayed γ -ray responses in intensity per 10^3 fission events as a function of time, with the effects of Compton scattering included, obtained for a pure samples of (a) ^{235}U and (b) ^{239}Pu after 1001 neutron pulses, are represented by the bold solid lines. The solid and dotted lines correspond to the contributions from ^{92}Kr and ^{137}I , respectively. The dashed line represents the cumulative contribution of all other nuclides that contribute to the total signal, but comprise less than 10% of the total signal in the temporal region extending from 0 to t_x s, where t_x is equal to 2.275 s.

due to improved statistics (i.e., increased intensity of the β -delayed γ -ray signal).

To explore the effect of the growth of longer-lived nuclides on the temporal dependence of the β -delayed γ -ray signal, the strongest contributing nuclides to the top ranked energy bin of 1216–1219 keV were determined for a Compton-included scenario after 1001 neutron pulses. This is illustrated graphically in Fig. 7 for pure samples of both (a) ^{235}U and (b) ^{239}Pu . The bold solid line represents the total signal and the solid and dotted lines correspond to the contributions from ^{92}Kr and ^{137}I , respectively. In contrast to the β -delayed γ -ray signal from pure ^{235}U after a single neutron irradiation, the ^{137}I represents a dominant contribution after 1001 neutron pulses. However, the contribution is roughly linear with time and thus, does not significantly contribute to the quantitative assessment. The dashed line represents the cumulative contribution of all other nuclides that contribute to the total signal, but comprise less than 10% of the total signal in the temporal region extending from 0 to t_x s. The contribution of longer-lived nuclides is non-linear at short time scales and more prominent after extended neutron irradiation and counting cycles (compare Fig. 7 with Figs. 2 and 6). The temporal dependence of the signal remains dominated by the contribution from ^{92}Kr . It is the difference in the temporal dependence of the β -delayed γ -ray signals from ^{235}U and ^{239}Pu that gives rise to the quantitative assessment and this difference, arising from the disparate fission fragment independent yields, is preserved.

5. Conclusions

The temporal dependence of the intensity of the delayed γ -ray signal in different energy bins provides novel isotopic-dependent signatures for the quantitative assay of ^{239}Pu and ^{235}U content in a mixed sample. However, the time-dependent effects of the Compton continuum serve to increase the uncertainty in the assay of the fractional ^{239}Pu sample content. Given that the relative intensities of β -delayed γ -rays of significantly different energies are not used for the determination of the fractional ^{239}Pu sample content, effects due to variation of detector efficiency or attenuation of the emitted γ -rays in the sample are minimized, effectively removing what was formerly one of the largest sources of systematic uncertainty in the conventional quantitative assay of complex samples (e.g., inhomogeneous samples containing multiple fissile nuclides [19]) using photon interrogation. In addition, it is not required that γ -decay lines are unobscured by other peaks, because the cumulative temporal response is comprised of the β -delayed

γ -ray signals emitted from several fission fragments and their decay daughters. Provided γ -rays are sufficiently penetrating to readily escape the sample, this innovative methodology can be applied to samples containing other fissionable isotopes. This means of analysis represents a first-order correction to the traditional spectral analysis of β -delayed γ -ray signatures and provides a potential pathway to the quantitative assay of ^{239}Pu content in spent fuel and for quantitative nuclear forensic applications. However, empirical validation of this methodology and experimental feasibility of the method using both pure and mixed samples of U–Pu must first be demonstrated.

Acknowledgments

The authors thank S.G. Prussin for fruitful discussions and advice. We gratefully acknowledge the contributions of R.D. Crabbs and J. Lorenzo. This work was supported, in part, by the University of California, Berkeley, Chancellor's Postdoctoral Fellowship Program, the Clare Boothe Luce Foundation, the Berkeley Nuclear Research Center (00F8F4 University of California Lab Fees Research Program, Award Number 09-LR-01-117616-VUJJ), the Next Generation Safeguard Initiative of the Office of Nonproliferation and International Security (US DOE, NA-241), the MPACT campaign of the FCR&D program of the Office of Nuclear Energy (US DOE), and the Director, Office of Science of the US Department of Energy at Lawrence Berkeley National Laboratory under contract number DE-AC02-05CHI1231.

References

- [1] S.J. Tobin, S.F. Demuth, M.L. Fensin, J.S. Hendricks, H.O. Menlove, M.T. Swinhoe, Determination of plutonium content in spent fuel with NDA – why an integrated approach? in: Annual Meeting of the Institute of Nuclear Material Management, Nashville, TN, July 2008, LA-UR-08-03763.
- [2] M.L. Felsin, S.J. Tobin, N.P. Sandoval, M.T. Swinhoe, H.O. Menlove, A Monte Carlo Based Spent Fuel Analysis Safeguards Strategy Assessment, Los Alamos National Laboratory Report No. LA-UR-09-01632, 2009.
- [3] A. Gavron, L.E. Smith, J.J. Ressler, Analysis of spent fuel assemblies using a lead slowing down spectrometer, Nucl. Instrum. Methods A 602 (2009) 581–587.
- [4] B.J. Quiter, B.A. Ludewigt, V.V. Mozin, S.G. Prussin, Nuclear resonance fluorescence for materials assay, IEEE Trans. Nucl. Sci. 58 (2011) 400–403.
- [5] E.B. Norman, S.G. Prussin, R.-M. Larimer, H. Shugart, E. Browne, A.R. Smith, R.J. McDonald, H. Nitsche, P. Gupta, M.I. Frank, T.B. Gosnell, Signatures of fissile materials: high-energy γ rays following fission, Nucl. Instrum. Methods A 521 (2004) 608–610.
- [6] M. Gmar, J.M. Capdevila, Use of delayed gamma spectra for detection of actinides (U,Pu) by photofission, Nucl. Instrum. Methods A 417 (1998) 841–845.
- [7] R.E. Marrs, E.B. Norman, J.T. Burke, R.A. Macri, H.A. Shugart, E. Browne, A.R. Smith, Fission-product gamma-ray line pairs sensitive to fissile material and neutron energy, Nucl. Instrum. Methods A 592 (2009) 463–471.
- [8] F. Carrel, M. Agelou, M. Gmar, F. Lainé, J. Loidon, J.-L. Ma, C. Passard, B. Poumarède, Identification and differentiation of actinides inside nuclear waste packages by measurement of delayed gammas, IEEE Trans. Nucl. Sci. 57 (2010) 2862–2871.
- [9] D.H. Beddingfield, F.E. Cecil, Identification of fissile materials from fission product gamma-ray spectra, Nucl. Instrum. Methods A 417 (1998) 405.
- [10] T.R. England, B.F. Rider, Evaluation and Compilation of Fission Product Yields, Los Alamos National Laboratory Report LA-UR-94-3106, ENDF-349, 1994.
- [11] M. Korun, Self-attenuation factors in gamma-ray spectrometry, Czech. J. Phys. 49 (1999) 429–434.
- [12] W.B. Wilson, S.T. Cowell, T.R. England, A.C. Hayes, P. Moller, A Manual for CINDER'90 Version 07.4 Codes and Data, LA-UR-07-9412 (December 2007, Version 07.4.2 updated March 2008).
- [13] R.B. Firestone, V.S. Shirley (Eds.), Table of Isotopes, eighth ed., vol. II, Wiley, New York, 1996.
- [14] B. Pritychenko, A.A. Sonzogni, Nucl. Data Sheets 109 (2008) 2822.
- [15] Evaluated Nuclear Structure Data File (6/21/2006), a computer file of evaluated experimental nuclear structure data maintained by the National Nuclear Data Center, Brookhaven National Laboratory.
- [16] M. Benedict, T.H. Pigford, H.W. Levi, Nuclear Chemical Engineering, second ed., McGraw-Hill, 1981 (Chapter 2).
- [17] G.F. Knoll, Radiation Detection and Measurement, third ed., John Wiley & Sons, 2000 (Chapter 4).
- [18] D.B. Pelowitz (Ed.), MCNPX User's Manual, Version 2.6.0, LA-CP-07-1473, April 2008; J.S. Hendricks et al., MCNPX 2.6.0 Extensions, LA-UR-08-2216, April 2008.
- [19] M.L. Fensin, S.J. Tobin, M.T. Swinhoe, H.O. Menlove, N.P. Sandoval, A Monte Carlo Based Spent Fuel Analysis Safeguards Strategy Assessment, LA-UR-09-01632, September 2009.